Anisotropic Photochemical Reactivity of Bulk TiO_2 Crystals

J. B. Lowekamp and G. S. Rohrer*

Department of Materials Science & Engineering, Carnegie Mellon University, Pittsburgh, Pennsylvania 15213-3890

P. A. Morris Hotsenpiller, J. D. Bolt, and W. E. Farneth

DuPont Company, Experimental Station, Wilmington, Delaware 19880-0356

Received: June 22, 1998; In Final Form: August 10, 1998

Polished and annealed surfaces of randomly textured rutile polycrystals were used to photochemically reduce Ag^+ to Ag metal in an aqueous solution. By correlating the surface orientations of more than 100 individual crystallites with the amount of deposited Ag, we conclude that the most reactive orientations lie near the {101} plane. Most annealed rutile surfaces are microscopically faceted so that they locally expose planes that are not parallel to the crystallite's average surface. The observations reported here indicate that the anisotropy of rutile's photochemical properties derives from differences in the properties of specific surface planes rather than the bulk crystallite orientation.

1. Introduction

Photochemical reactions catalyzed by titania surfaces can be used to degrade dilute impurities in air and water.[1−3] In a recent paper, we described the influence of surface orientation on the photochemical reactivity of thin rutile epilayers.[4] Briefly, we found that films with {001}, {101}, and {111} orientations were approximately an order of magnitude more photocatalytically reactive than those with {100} and {110} orientations. Furthermore, quantum yield measurements indicate that the anisotropic reactivity of the films is related to differences in the efficiency of electron−hole pair utilization rather than electron−hole pair creation. This observation might have considerable practical importance for the design of optimized photocatalyst microstructures. The objective of the current report is to demonstrate that the anisotropic reactivity reported earlier for thin film samples also occurs on the surfaces of bulk samples and that the anisotropy of the photoactivity depends on the exposed surface planes rather than the bulk orientation.

The experiments described here have been conducted on polycrystalline ceramics composed of individual crystallites approximately 55 μm in diameter. Polished and annealed surfaces of such ceramics provide a wide range of surface orientations in close proximity. When the polycrystal is immersed in aqueous $AgNO_3$ solution and exposed to light, the surface catalyzes the photoreduction of Ag^+ to Ag metal, which deposits as islands on the surface.[5,6] By correlating the amount of photoreduced Ag found on individual surfaces to the crystallite orientation, we find that surfaces containing {101} facets are far more reactive than others.

2. Experimental Procedures

The experiments described here were conducted on polycrystalline (rutile) TiO_2 ceramics fabricated in the following way. TiO_2 powder was uniaxially compacted under 140 MPa to form disk-shaped pellets with an approximate diameter of 11 mm and a thickness of 2.5 mm. The pellets were then enclosed in latex and isostatically pressed under 280 MPa. After compaction, the samples were placed in an alumina crucible with an excess quantity of the parent powder so that the pellets did not come into contact with the crucible. The samples were heated to 1600 °C at 5 °C/min in air, annealed at 1600 °C for 24 h, and then cooled at 5 °C/min. The cream-colored, sintered samples were then separated from the packing powder and ground and polished with diamond grits down to 0.25 μm to produce a flat surface. After polishing, the samples were thermally etched in air at 1200 °C for 4 h to remove polishing damage, facet the surfaces, and produce grooves at the grain boundaries. The average grain size was 55 μm, and the samples exhibited some intra- and intergranular porosity. Both the starting powder and the final ceramic (after sintering, polishing, and grooving) were analyzed for Al, Fe, and Si by flame emission spectroscopy. The starting powder contained 13 ppm Al, less than 10 ppm Fe, and 40 ppm Si. The sintered ceramic contained 11 ppm Al, less than 10 ppm Fe, and 100 ppm Si. The accumulation of Si in the ceramic probably occurred during handling and firing.

The surface morphology of approximately 100 contiguous grains was examined in the ambient using an atomic force microscope (Park Scientific Instruments). The microscope was operated in the contact mode using high aspect ratio Si ultralevers and constant forces in the 0.1−5 nN range. After the structure of the clean, annealed surfaces was characterized, the relative photoactivity of each grain was assumed to be proportional to the amount of Ag^+ photoreduced to Ag metal when illuminated by UV radiation for a fixed time. On a macroscopic scale, the deposition of silver islands leads to a darkening of the surface. The reduction in the reflected light intensity that occurs during silver deposition was continuously measured with a previously described apparatus and used to determine the samples' average photoactivity.[4]

Briefly, the samples were covered with a 2.5 mm deep 0.1 N $AgNO_3$ solution contained by an O ring and a glass cover

* To whom correspondence should be addressed. Phone: 412-268-2696. Fax: 412-268-7596. E-mail: gr20+@andrew.cmu.edu. www: http://neon.mems.cmu.edu/rohrer.html.

S1089-5647(98)02721-7 CCC: $15.00
Published on Web 08/29/1998

slip and placed on a microscope stage. The samples were illuminated with a 100 W high-pressure mercury lamp through a 10× objective lens. The formation of metallic silver was apparent by a darkening of the exposed area. The samples were illuminated until the reflected intensity at 550 nm decreased by 4 to 8%. For example, the sample described in detail here was illuminated for 7.5 min until the reflected intensity decreased by 8%. Following this treatment, the samples were rinsed in distilled water, dried, and re-examined by atomic force microscopy (AFM).

After the AFM imaging was completed, the crystallographic orientations of the grains were determined from electron backscattered diffraction patterns (EBSP).[7,8] The samples were imaged (uncoated) in a Phillips XL40FEG scanning electron microscope. Using fiducial marks on the sample, the grains examined by AFM were located and an EBSP was obtained for each grain. The patterns were indexed using Orientation Imaging Microscopy Software, version 2.5 (TexSEM Laboratories, Inc.), which returned a set of Euler angles (ϕ_1, Φ, ϕ_2) for each grain. The Euler angles specify the orientation relationship between the sample reference frame and the crystallographic axes.[8] From these data, the components of the surface normals can be computed. While this report focuses on data from a single experiment, the results described here are characteristic of three similar experiments performed to ensure reproducibility.

3. Results

The AFM images in Figure 1 show the same area of the surface before and after the treatment in aqueous $AgNO_3$. In these topographic images, the contrast arises from vertical height differences on the surface, where black is low and white is high. For example, the dark contrast in Figure 1a marks the thermal grooves at the grain boundaries and pores that intersect the surface. The image in Figure 1b shows that features raised above the surface level (white contrast) have appeared after the reaction. Some grains appear to be uniformly coated, while others exhibit an inhomogeneous distribution of elevated features. In unilluminated regions of the specimen, there are no noticeable changes on any of the grains. On the basis of energy-dispersive X-ray spectroscopy (Oxford Isis) conducted in a scanning electron microscope (Phillips XL30FEG), there is a one-to-one correlation between the elevated regions of white contrast and high concentrations of Ag. Therefore, we conclude that the elevated surface features that formed during the UV exposure are islands of silver metal. The fact that silver deposits under these conditions has been known for many years.[5,6]

On the basis of our observations of more than 100 grains, we distinguish three types: those that are very reactive, those that are moderately reactive, and those that are relatively unreactive. An example of each type of grain is illustrated in Figure 2, where AFM images show the same triple junction before and after the reaction. The very reactive grains are uniformly covered with Ag islands so that the morphology of the unreacted surface can no longer be distinguished. As an example, note the grain in the upper left part of the images in Figure 2. The moderately active grains have easily observable silver islands, while the morphology of the TiO_2 surface remains visible. An example of a moderately active grain is illustrated in the lower left part of the images in Figure 2. A higher resolution image of this surface, before and after the reaction, is shown in Figure 3. The diagonal lines on the surface correspond to steps with an average height of 33 nm and the equiaxed features with lighter contrast in Figure 3b are the silver

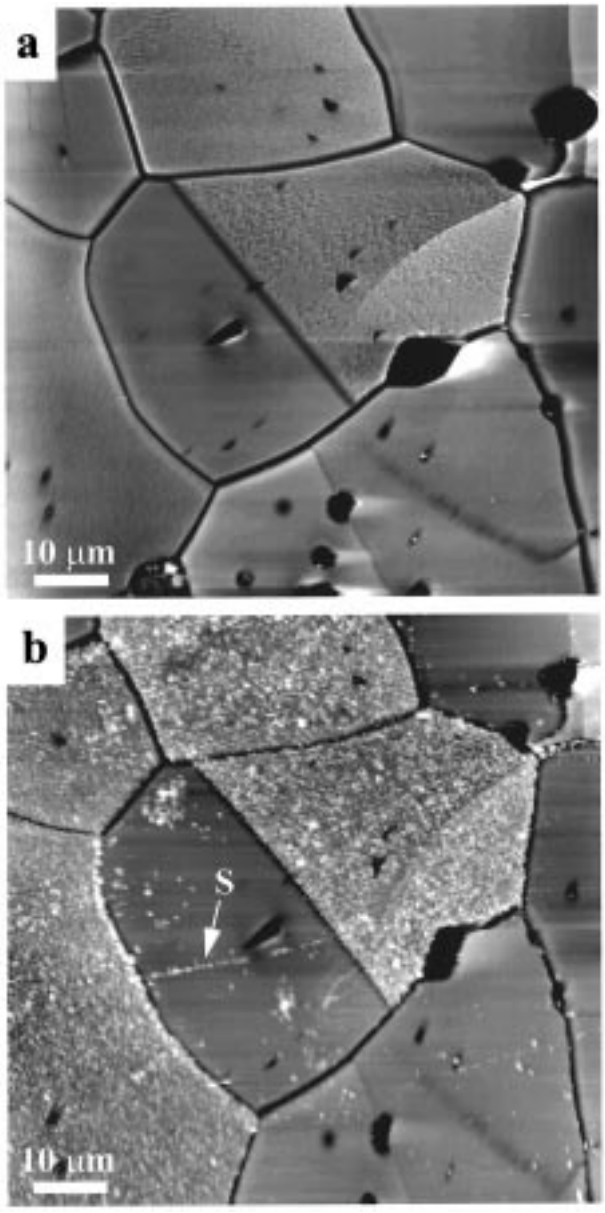

Figure 1. AFM images of the same area of a thermally etched TiO_2 ceramic surface before (a) and after (b) the photochemical deposition of silver. The black-to-white vertical contrast is 230 nm (a) and 330 nm (b).

islands. The relatively unreactive grains have an inhomogeneous distribution of silver, as exemplified by the grain on the right-hand side of the images in Figure 2. While parts of the unreactive grain in the vicinity of grain boundaries, residual polishing scratches, pores, and other defects do show deposited silver, the flat regions of the surface are indistinguishable before and after the reaction. It is the heterogeneous distribution of Ag that distinguishes the relatively unreactive grains from the moderately reactive grains. The inhomogeneous deposition is clearly illustrated by the relatively unreactive grain near the center of the images in Figure 1. Note that in the image in Figure 1b Ag islands have preferentially deposited in a straight line at the polishing scratch labeled "S".

The data in Figure 4 illustrate the correlation between the crystallographic orientation and the reactivity of the individual grains. Because of rutile's tetragonal symmetry ($P4_2/mnm$), we only need to consider a limited range of orientation space where each family of indistinguishable planes, written as {*hkl*}, is represented by a single plane, written as (*hkl*). Considering the

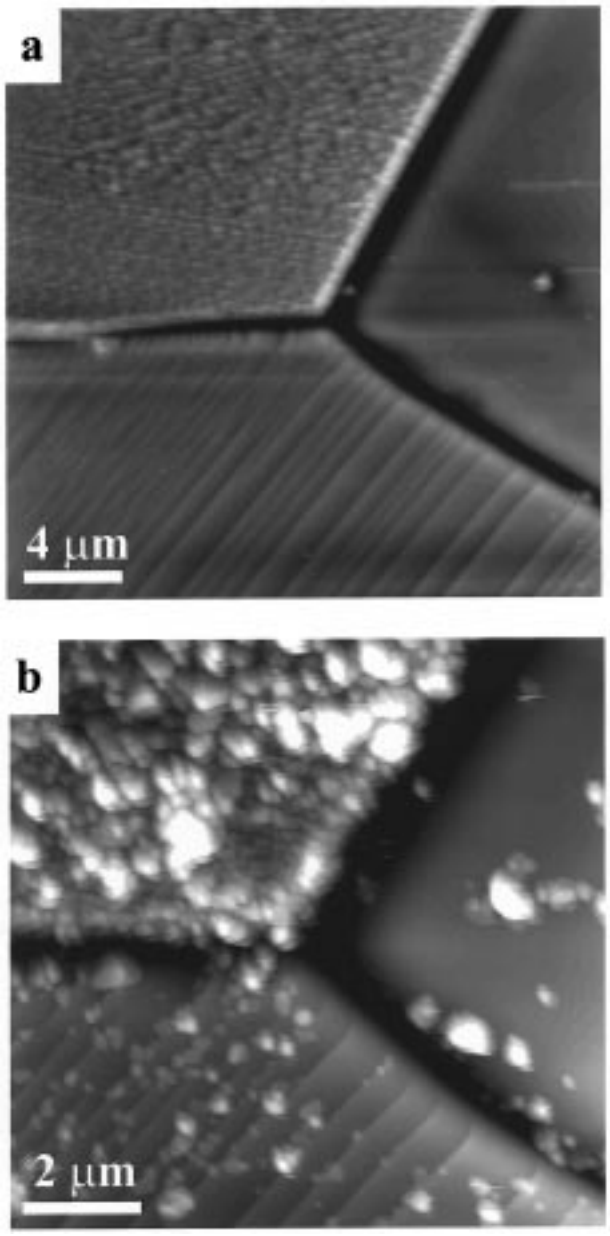

Figure 2. AFM images of the same area of a thermally etched TiO_2 ceramic surface before (a) and after (b) the photochemical deposition of silver illustrating a low-reactivity grain (right), a moderately reactive grain (lower left), and a very reactive grain (upper left). The black-to-white vertical contrast is 150 nm (a) and 250 nm (b). While the two images show the same triple junction, note the difference in the lateral scale.

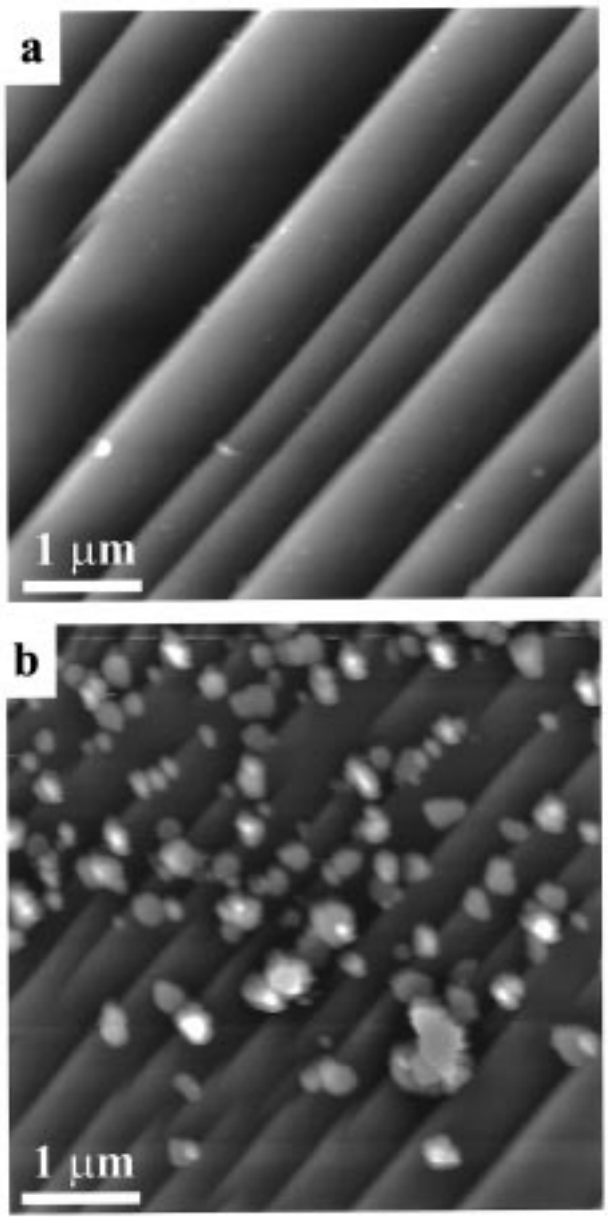

Figure 3. AFM images of the same grain surface (although not the same location) on a thermally etched TiO_2 ceramic surface before (a) and after (b) the photochemical deposition of silver. This particular grain is the moderately active grain shown in Figure 2. The steps in (a) are oriented in the [111] direction, and the black-to-white vertical contrast is 48 nm. The black-to-white vertical contrast in (b) is 120 nm and the silver islands are 30−100 nm high.

symmetry, the normals to all distinguishable planes intersect a triangular area on the surface of a sphere; the normals to the (001), (010), and (110) planes mark the vertexes of this unit triangle. A stereographic projection of the unit triangle and the observed surface normals is shown in Figure 4. Inspection of the distribution leads to the conclusion that grains with orientations between {101}, {001}, and {111} are more reactive than those closer to {110} and {100}.

4. Discussion

The anisotropy of the photochemical reactivity observed on the bulk rutile surface is consistent with what we reported earlier for thin films. We found that surface orientations near {001}, {111}, and {101} have a greater photoactivity than those near {110} and {100}. However, by examining a wider range of orientations, it appears that the most reactive orientations occur closer to {101} than to {111} or {001}. Note especially that the orientations closest to {001} and {111} are moderately reactive and unreactive, respectively, rather than very reactive.

The potential sources for the anisotropic reactivity can be separated into two categories: those relating to the structure and chemistry of the uppermost atomic layers of the sample and those relating to bulk processes such as the absorption of light, charge transport, and the subsurface space charge layer. The observations presented here indicate that the surface characteristics are more important than the bulk orientation. For example, consider the fact that on crystals with unreactive bulk orientations, silver precipitates still form on the localized out-of-plane components of the surface in the vicinity of grain boundary grooves and near residual polishing scratches. On moderately reactive surfaces, the silver islands are frequently

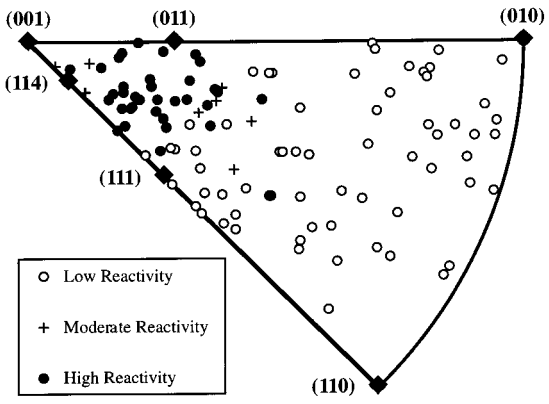

Figure 4. Relative reactivity as a function of surface orientation. Each point in the stereographic projection represents an observed grain orientation (surface normal). The surface normals of reactive grains are indicated by solid circles, the unreactive grains are indicated by empty circles, and moderately reactive grains are indicated by crosses. The diamonds represent the locations of the normals to low-index planes. On the basis of the Euler angles for each grain, the radial coordinate is $\tan(\Phi/2)$ and the angular coordinate, from the [010] axis, is ϕ_2.

observed to grow on only one of the available facets. If the differences in reactivity were a purely bulk phenomenon, local topographic variations would not greatly influence the absorption of photons or the transport of charge to the surface. This leads us to consider the detailed morphological structure of the grain surfaces.

Because of its anisotropic surface energy, randomly oriented rutile surfaces will not always have a planar configuration. Although the polished surfaces begin flat, the existence of neighboring facets with lower relative energies frequently leads to an increase in the total surface area as the planar surface relaxes into low-energy facets during high-temperature annealing.[9−12] Therefore, it is important to consider not only the bulk orientation but also the indices of the facets that make up the surface and the lines and corners where they meet.

We begin by classifying all grain surfaces as being faceted or unfaceted. However, it is important to clarify the distinction between these two categories. AFM images reveal steps as small as a few angstroms. Considering the fact that all real surfaces have some steps and that a facet is really nothing more than a stack of very closely spaced steps, one needs to differentiate between steps and facets. We will arbitrarily distinguish steps from facets by saying that a facet is a step that is at least five times as high as the longest lattice parameter. In this case, features higher than 23 Å are called facets, and features below this height are called steps. Using this distinction, we can say that all of the reactive and moderately reactive grains are faceted. While many of the unreactive grains are classified as unfaceted, others are also faceted. Therefore, the increase in specific surface area that accompanies faceting does not by itself explain the increased reactivity.

Instead, the important point seems to be the identity of the facets. According to our observations, the primary low-index facets formed on rutile surfaces are {101} and {111} at one end of the unit triangle and {110} and {100} at the other end. Between these two limits, there is apparently a continuous range of stable higher index orientations. These observations are consistent with previous studies of surface energy and faceting of rutile.[9−12] However, it is important to recognize that kinetic limitations frequently influence such observations. Of the 37 grains classified as very reactive, 34 had identifiable {101} facets and the remainder had higher index orientations. Orientations near {111} were not faceted, indicating that this surface is stable. However, contrary to our results from films, this orientation is relatively unreactive with respect to {101}. One possible explanation for this inconsistency is that the films with {111} orientation were rough and contained a high fraction of out-of-plane surfaces. As one tilts away from {111}, the reactivity increases, presumably because of the appearance of active {101} facets. The unreactive grains are composed of {110}, {100}, and higher index orientations.

In light of these observations, it is interesting to consider potential local structures for the relevant surfaces. The Ti atoms in rutile are octahedrally coordinated by O in the bulk. If we assume ideal bulk terminations, the Ti atoms on the {100} surfaces are five-coordinate, and steps can be created along the *c* axis or along the perpendicular in-plane direction without decreasing the Ti coordination number below five. Half of the Ti on the {110} surfaces are five-coordinate, while the remainder retain their full complement of oxygen. The creation of steps along the *c* axis direction creates five-coordinate Ti, while steps along the perpendicular direction leave some Ti in fourfold coordination. On the {101} surfaces, all Ti are five-coordinate, but forming steps in any direction creates four-coordinate Ti. The {111} surfaces have a mixture of three- and five-coordinate Ti, and steps in any direction create four-coordinate Ti. There are higher index planes near {111} that are also thought to be stable (such as {114}) that contain a mixture of four- and five-coordinate Ti.

In summary, one structural feature that is more abundant on reactive surfaces than on unreactive surfaces is the four-coordinate Ti. For the inactive orientations, this species only occurs along steps on {110} surfaces that have a component perpendicular to the *c* axis. However, for orientations near {101} and {111}, this species occurs at almost all steps and even on the planes of some of the higher index surfaces. In earlier studies of reactions on TiO_2 surfaces, Barteau and coworkers[13−16] found that surfaces containing four-coordinate Ti had an increased selectivity for certain partial oxidation reactions. More recently, it has been observed that molecular dispersions of tetrahedrally coordinated Ti photocatalytically decompose NO to N_2, O_2, and N_2O, while aggregated octahedrally coordinated Ti shows a high selectivity for the production of N_2O.[17] In the present case, this special geometry might increase the reactivity either by altering the efficiency with which carriers are trapped at the surface or by altering the rate at which photogenerated carriers are transferred across the solid−liquid interface. For example, it is possible that the relatively electron-rich surface O surrounding the four-coordinate Ti are more effective hole traps than those surrounding five-coordinate metal sites.[18] Similarly, a surface Ti with four O neighbors might bind adsorbed species from the solution more effectively, and this could promote charge transfer from the crystal to the adsorbate. However, the existence of tetrahedrally coordinated Ti on the surfaces of finely divided TiO_2 powders remains questionable. Recent XAFS results suggest that the Ti on the surfaces of particles with diameters as small as 30 Å remains octahedrally coordinated.[19] If four-coordinate Ti are the key structural feature on active surfaces, one would expect the reactivity to increase continuously with the density of steps as the surface orientation changes from (110) to (011) by a rotation around the *a* axis. In future work, we plan to explore this transition region in greater detail.

5. Conclusion

By correlating the photochemical reactivity of more than 100 individual crystallites with their orientations, we conclude that the most reactive surfaces on rutile are near the {101} orientation. Furthermore, characterization of the microscopic facets on each grain surface leads us to conclude that the anisotropy of rutile's photochemical properties derives from differences in the properties of specific surface planes rather than the bulk crystallite orientation.

Acknowledgment. Primary support for this work was provided by a National Science Foundation GOALI supplement (DMR-9712606) to YIA Grant DMR-9458005. This work was supported in part by the MRSEC Program of the National Science Foundation under Award Number DMR-9632556 and made use of MRSEC Shared Experimental Facilities supported by the same award.

References and Notes

(1) Ollis, D. F. *Environ. Sci. Technol.* **1985**, *19*, 480.
(2) Ollis, D. F.; Pelizzetti, E.; Serpone, N. *Environ. Sci. Technol.* **1991**, *25*, 1523.
(3) Wold, A. *Chem. Mater.* **1993**, *5*, 280.
(4) Morris Hotsenpiller, P. A.; Bolt, J. D.; Farneth, W. E.; Lowekamp, J. B.; Rohrer, G. S. *J. Phys. Chem. B* **1998**, *102*, 3216.
(5) Clark, W. C.; Vondjidis, A. G. *J. Catal.* **1965**, *4*, 691.
(6) Herrmann, J.-M.; Disdier, J.; Pichat, P. *J. Catal.* **1988**, *113*, 72.
(7) Adams, B. L.; Wright, S. I.; Kunze, K. *Met. Trans.* **1993**, *24A*, 819.
(8) Randle, V. Microtexture Determination and its Applications; The Institute of Materials: London, 1992.
(9) Firment, L. *Surf. Sci.* **1982**, *116*, 205.
(10) Kurtz, R. L. *Surf. Sci.* **1986**, *177*, 526.
(11) Poirier, G. E.; Hance, B. K.; White, J. M. *J. Vac. Sci. Technol.* **1992**, *B10*, 6.
(12) Ramamoorthy, M.; Vanderbilt, D.; King-Smith, R. D. *Phys. Rev. B* **1994**, *49*, 16721.
(13) Kim, K. S.; Barteau, M. A. *Surf. Sci.* **1989**, *223*, 13.
(14) Kim, K. S.; Barteau, M. A. *J. Catal.* **1990**, *125*, 353.
(15) Idriss, H.; Pierce, K.; Barteau, M. A. *J. Am. Chem. Soc.* **1991**, *113*, 715.
(16) Lusvardi, V. S.; Barteau, M. A.; Farneth, W. E. *J. Catal.* **1995**, *153*, 41.
(17) Yamashita, H.; Ichihashi, Y.; Anpo, M.; Hashimoto, M.; Louis, C.; Che, M. *J. Phys. Chem.* **1996**, *100*, 16041.
(18) Micic, O. I.; Zhang, Y.; Cromack, K. R.; Trifunac, A. D.; Thurnauer, M. C. *J. Phys. Chem.* **1993**, 97, 7277.
(19) Chen, L. X.; Rahj, T.; Wang, Z.; Thurnauer, M. C. *J. Phys. Chem. B* **1997**, *101*, 10688.